Catalysis Science & Technology

One-Step Production of Renewable Adipic Acid Esters from Mucic Acid over an Ir-ReOx/C Catalyst with Low Ir Loading

Journal:	*Catalysis Science & Technology*
Manuscript ID	CY-ART-06-2022-001144.R1
Article Type:	Paper
Date Submitted by the Author:	17-Oct-2022
Complete List of Authors:	Jang, Jun Hee; University of California Santa Barbara, Chemical Engineering Hopper, Jack; University of California Santa Barbara, Chemistry and Biochemistry Ro, Insoo; University of California Santa Barbara, Chemical Engineering Christopher, Phillip; University of California Santa Barbara, Abu-Omar, Mahdi; University of California Santa Barbara, Chemistry and Biochemistry, and Chemical Engineering

Catalysis Science & Technology

ROYAL SOCIETY OF CHEMISTRY

PAPER

View Article Online
View Journal | View Issue

One-Step Production of Renewable Adipic Acid Esters from Mucic Acid over an Ir-ReO_x/C Catalyst with Low Ir Loading

Jun Hee Jang[a,†], Jack T. Hopper[b,†], Insoo Ro[a,c], Phillip Christopher[a,*], Mahdi M. Abu-Omar[a,b,*]

Abstract

The production of adipic acid, a large-volume platform chemical, from biomass represents a petroleum-free route to manufacturing nylon and other polymers more sustainably. In this study, a one-step conversion of bioderived mucic acid to adipates is reported over a heterogeneous, bifunctional Ir-ReO_x/C catalyst via deoxydehydration (DODH) and catalytic transfer hydrogenation (CTH) using isopropanol as a green solvent and reductant. With very low loading Ir content (0.05 wt%), the catalyst provides a low-cost option for the tandem DODH-CTH process, while still enabling reuse and regeneration for at least five cycles. The reported catalytic system generates adipates in good yield (63%) without the need for additives (acids or halogens), or high pressure H_2. Through model reactions and spectroscopic analyses, a bifunctional DODH-CTH mechanism was supported, with the $Re^{VI/IV}$ redox pair as active DODH species and Ir^0 saturating the dialkene intermediate via CTH. Thermal treatment in catalyst preparation and regeneration was optimized to limit metal leaching while maintaining good activity. The present work outlines a one-step deoxygenation of an aldaric acid substrate from biomass using a bimetallic catalyst of low noble metal content to an important monomer for the polymer industry. This system facilitates use in future syntheses of sustainable chemicals from renewable oxygenates where the catalyst is reusable and affordable.

1. Introduction

Lignocellulosic biomass is an attractive substitute to petroleum-based feedstocks for the production of fuels and commodity chemicals due to its sustainability and global ubiquity.[1,2] One such process that can benefit from improved sustainability by utilizing biomass as a feedstock is the production of adipic acid. A C6 dicarboxylic acid, adipic acid is primarily used in the production of nylon-6,6 (approximately 75%), with additional utilities as a plasticizer and polyurethane precursor.[3] As a result, adipic acid represents a high-value chemical, produced in excess of 3.5 Mt per year with an annual growth rate of 3-5%.[4,5] Globally, the market for adipic acid is projected to be in excess of $8 billion by 2025.[5]

Pressing issues in adipic acid production are centred around its negative environmental impacts, due to a petroleum-based starting material and generation of harmful emissions.[6] Benzene, a known carcinogen derived from petroleum, is the primary industrial precursor used in the production of adipic acid and makes the resulting process dependent on a non-renewable feedstock.[6] After hydrogenation and subsequent oxidation to yield a cyclohexanol-cyclohexanone mixture ('KA-oil', <10% yield), nitric acid is used in an oxidative ring-opening to form adipic acid.[7,8] This final step results in the evolution of nitrous oxide (N_2O), a potent greenhouse gas, whose release from adipic acid production constituted approximately 15% of the CO_2 equivalents emitted from the entirety of U.S. petrochemical production in 2015.[9,10]

Renewable, less-emissive, and more sustainable production of adipic acid via glucose and its derivatives has been extensively studied. Utilizing a biocatalytic pathway, Boles and co-workers reported the bacterial synthesis of *cis*,*cis*-muconic acid via glucose,[11] which can be readily hydrogenated to yield adipic acid. In an analogous fashion from lignin, a modified version of *Pseudomonas putida* was used to convert lignin-derived phenols into muconic acid intermediate. After treatment with Pd/C at 24 bar H_2, adipic acid was produced in good yield (72%).[12] Unfortunately, to date, the biocatalytic route is limited by low initial substrate concentrations and long reaction times (>100 h). Alternatively, chemocatalytic routes have been demonstrated via glucose derivatives 2,5-furandicarboxylic acid,[13] tetrahydrofuran 2,5-dicarboxylic acid,[14,15] glucaric acid,[16] or the latter's corresponding lactone.[17] Reported by Vlachos and Xu et al., the conversion of tetrahydrofuran 2,5-dicarboxylic acid into adipic acid was achieved over zeolites using NaI and propionic acid.[14] These studies produce higher yields than

[a] *Department of Chemical Engineering, University of California Santa Barbara Santa Barbara, California 93106 United States E-mail: abuomar@chem.ucsb.edu, pchristopher@ucsb.edu*
[b] *Department of Chemistry and Biochemistry University of California Santa Barbara Santa Barbara, California 93106 United States*
[c] *Department of Chemical and Biomolecular Engineering Seoul National University of Science and Technology Seoul 01811, Republic of Korea*
† *Co-first author*
Electronic Supplementary Information (ESI) available: [details of any supplementary information available should be included here]. See DOI: 10.1039/x0xx00000x

biocatalytic pathways, but still require the use of halogens, organic acids, or molecular H_2, often at high pressures.[18]

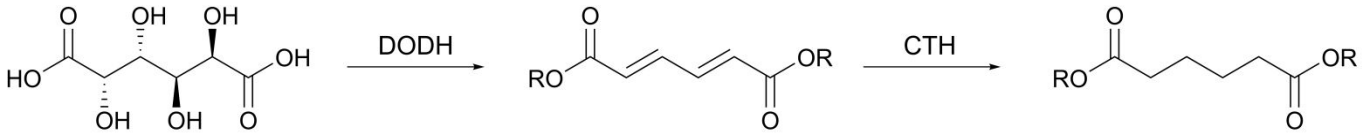

Scheme 1. Tandem DODH-CTH pathway of mucic acid to adipic acid/adipates via muconic acid

Deoxydehydration (DODH), followed by alkene saturation through direct hydrogenation or catalytic transfer hydrogenation (CTH) is an efficient and sustainable route to adipic acid/adipates from mucic acid (galactaric acid), as shown in Scheme 1. A member of the aldaric acids, mucic acid can be produced via oxidation of galactose from biomass.[19] High-valent rhenium catalysts in the presence of reductants have been extensively studied for DODH on many different substrates, including biomass-derivatives.[17,20] In a one-pot procedure, 62% yield of adipates was achieved by Toste and Shiramzu via mucic acid using homogenous perrhenic acid ($HReO_4$) and subsequent hydrogenation over Pd/C.[21] Via a similar two-step reaction, a 99% yield of adipates was obtained by using 3-pentanol as a reductant for DODH catalyst methyltrioxorhenium (CH_3ReO_3), p-Toluenesulfonic acid (TsOH) as an acid additive, and Pt/C serving to saturate the intermediate dialkene.[22] Though high-yielding, these systems require homogeneous Re which would complicate scale-up due to challenges in separation and recycling of these high-cost catalysts.[23] Therefore, it is becoming vital to develop a reusable heterogeneous rhenium catalyst for DODH, which could also have the added benefit of increased stability at high temperatures.[24,25]

To this end, Likozar et al. screened a variety of homogeneous and heterogeneous Re catalysts with various supports with and without hydrogenation catalyst for the conversion of mucic acid to adipic acid.[25] Our group recently reported a bifunctional Pt-ReO_x/C catalyst for both DODH and CTH with isopropanol as hydrogen donor and solvent. The system achieved a one-step conversion of mucic acid to adipates with high yield (85%) in 24 h and the subsequent hydrolysis step produced 77% yield of isolated adipic acid.[26] However, these systems require a high amount of noble metals (Pt or Pd) for hydrogenation (1–2 mol% relative to the substrate). These catalysts, especially those active for hydrogenation, comprise a significant amount of the total process cost and remain the central barrier to large-scale adoption of heterogeneously-catalyzed adipic acid production.[23] The noble metals such as Ru, Pt, Rh and Ir are also at high supply risk from increased use (**Figure 1**). Therefore, we were motivated to reduce the noble metal loading in order to increase the economic viability and sustainability of the resulting process.

In this study, we first synthesized three monometallic DODH catalysts (MoO_x, VO_x, and ReO_x) supported on activated carbon to examine their effectiveness in DODH of mucic acid. To saturate the resulting alkene(s) intermediates by CTH, several bifunctional M-ReO_x/C catalysts were synthesized with various hydrogenation metals, M, at very low loading (0.05 wt%). The use of Ir with ReO_x/C presented the highest yield of CTH products when compared to other hydrogenation metals, including Pt and Pd. A 63% yield of adipates was attained over the bifunctional catalyst Ir-ReO_x/C in isopropanol as solvent and reductant for both DODH and CTH reactions. By significantly lowering the Ir metal content to 0.05 wt%, a marked decrease in catalyst cost was achieved in comparison to previous reports of mucic acid DODH-CTH, reducing the cost per mol product by at least one order of magnitude in many cases (**Table S1**). A catalytic mechanism for DODH-CTH over Ir-ReO_x/C is proposed based on observed reactivity and XPS analysis. Additionally, catalyst recycling, regeneration conditions, and stability are presented.

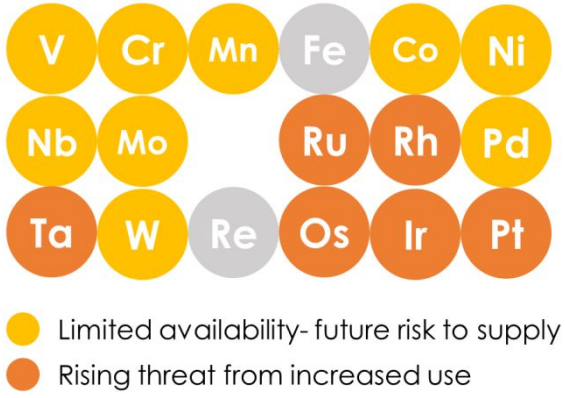

Figure 1. Select endangered transition elements that are commonly used as catalysts. Source: ACS Green Chemistry Institute, Endangered Elements 2019.

2. Experimental

2.1 Catalyst preparation. The monometallic 5 wt% ReO_x/C catalyst was prepared by a wet impregnation of activated carbon (Sigma-Aldrich) with ammonium perrhenate(VII) (NH_4ReO_4) (Strem Chemicals) aqueous solution. 1 g of activated carbon was added to 4 mL of ammonium perrhenate aqueous solution (50 mg Re) and stirred for 3 h. Water was evaporated in a preheated 80°C oil bath for 1.5 h, after which the residue was dried in a 120°C oven overnight. The catalyst was thermally treated at 480°C under an N_2 flow (40 ccm) for 4 h. 5 wt% MoO_x/C, 5 wt% VO_x/C, and

0.05 wt% Ir/C catalysts were prepared by the same procedure with aqueous solutions of ammonium molybdate(VI) (Acros Organics), ammonium metavanadate(V), and iridium(III) chloride (Sigma Aldrich). Bimetallic M–ReO_x/C (0.05 wt% M and 5 wt% of Re, M = Ni, Pd, Ru, Rh, Pt, and Ir) catalysts were synthesized via co-impregnation of activated carbon with the appropriate amount of aqueous solutions of ammonium perrhenate and metal precursor. Hexachloroplatinic(IV) acid, nickel(II) nitrate, tetraaminepalladium(II) nitrate, iridium(III) chloride (Sigma-Aldrich), tris-(ethylenediamine)rhodium(III) chloride (Alfa Aesar), ruthenium(III) nitrosyl nitrate (Acros Organics) were used as metal precursors. After evaporating water in an 80°C oil bath and subsequently drying at 120°C overnight, thermal treatment of the catalysts was conducted at the same conditions as above (N_2/480°C/4 h).

2.2 Catalyst characterization. To quantify the amount of metals present on the catalysts after reaction and various thermal treatment temperatures, inductively coupled plasma-absorption emission spectroscopy (ICP-AES) analysis was conducted using a Thermo iCAP 6300 instrument. To prepare the catalyst sample for ICP analysis, 2.3 mL aqua regia was used to digest metallic species present in 20 mg Ir-ReO_x/C catalyst by refluxing for 6 h at 150°C. After 6 h, the solution was allowed to cool, filtered, and diluted to 50 mL with distilled water. X-ray diffraction (XRD) spectra were recorded using a PANalytical Empyrean X-ray diffractometer using Cu Kα radiation (λ = 0.154 nm) in 2θ span of 5-80° to determine presence of crystalline species.

High-angle annular dark-field scanning transmission electron microscopy (HAADF-STEM) images were acquired using a Thermo Scientific Talos G2 microscope operating at 200 kV. The samples were diluted in ethanol and transferred to a carbon film copper grid to prepare for imaging. Additionally, an energy-dispersive X-ray spectroscopy (EDX) Super-X detector was used to map the elemental distribution of Re, Ir, and C.

X-ray photoelectron spectroscopy (XPS) analysis was carried out with a ThermoFisher Escalab Xi+ instrument using an Al Kα monochromatic X-ray source. Ir 4f, Re 4f, and C 1s spectra were recorded at 20eV in high-resolution. All of the recorded spectra were calibrated by setting the binding energy of the peak of C 1s to 284.5 eV and peaks were deconvoluted using CasaXPS software. The fresh, spent, and regenerated Ir-ReO_x/C catalysts were handled in air before transfer to the XPS chamber and the fresh sample was analyzed without additional treatment after preparation as described previously.[26] For *in-situ* analysis, the catalyst was transferred to a glovebox under N_2 atmosphere, mounted on a transfer vessel, and transported to the XPS chamber in order to avoid exposure to air.

Thermogravimetric analysis (TGA) was carried out with a Discovery TGA instrument to determine the presence of organic deposits via analysis of mass loss with temperature of fresh, spent, and regenerated catalysts. TGA analysis began at 50°C and samples were heated at a rate of 20°C/min until 100°C was reached. 100°C was then maintained, isothermally, for 5 minutes to remove physisorbed water after which the samples were heated to a final temperature of 600°C at 20°C/min.

2.3 General catalytic procedure. DODH-CTH tandem reaction of mucic acid was conducted in a 75 mL Parr batch reactor. The Ir-ReO_x/C catalyst (150 mg, 5 wt% Re and 0.05 wt% Ir) was loaded with mucic acid (1 mmol, 210 mg) and isopropanol (40 mL) in the Parr vessel. The vessel was pressurized with nitrogen to 15 bar and then heated to the reaction temperature. After reaction, the spent catalyst was filtered, washed with pure isopropanol (30 mL), and dried in a 120°C oven overnight. The reaction solution was then concentrated under reduced pressure. The concentrated products were dissolved in d_6-DMSO (Cambridge Isotope Laboratories) and analyzed by NMR with benzaldehyde (Sigma-Aldrich) as an internal standard. ^{1}H NMR and ^{13}C NMR spectra were acquired on an Agilent Technologies 400 MHz, 400-MR DD2 spectrometer.

2.4 Stability test. Due to its chemical similarity to mucic acid and excellent solubility in isopropanol, diisopropyl L-(+)-tartrate (Tokyo Chemical Industry) was selected as a substrate for stability tests. Upon DODH of diisopropyl L-(+)-tartrate, diisopropyl fumarate (Tokyo Chemical Industry) is formed and CTH of diisopropyl fumarate yields diisopropyl succinate (Tokyo Chemical Industry). For the initial test, 2 mmol substrate, 50 mg Ir-ReO_x/C catalyst (mixed with 100 mg activated carbon), and 20 mL isopropanol were loaded into the reaction vessel, which was subsequently pressurized to 15 bar of N_2. The vessel was allowed to heat to 220°C, upon which the reaction time was started. After reaction completion at 20 min, the vessel was quenched in an ice bath. The used catalyst was separated via filtration, washed with 30 mL isopropanol, and dried in an oven overnight at 120°C. During each recycling, a small amount (4-10 mg) of catalyst was lost. The amount of substrate and solvent used in subsequent recycling steps was calculated based on the amount of the recovered catalyst in each step. The recycled catalyst was used in a subsequent catalytic test without regeneration (denoted hereafter as "spent") and with a regeneration step ("regenerated") by reoxidation at 300°C for 4 h under flowing air.

3. Results and discussion

3.1 Catalyst screening. The possibility of substituting more expensive rhenium-based catalysts with molybdenum or vanadium-based catalysts for DODH was first explored. Molybdenum and vanadium-based catalysts have garnered much attention as an alternative to rhenium-based catalysts for DODH despite their lower efficiencies.[20,27,28] ReO_x/C, VO_x/C, and MoO_x/C were prepared by impregnation and compared for their reactivity in DODH. Activated carbon was chosen for support because carbon-supported ReO_x catalysts exhibited high DODH selectivity, while acidic materials such as Al_2O_3 were found to catalyze side reactions, impeding DODH activity and leading to poor selectivity.[25] Additionally, screenings by Palkovits et al. revealed maximum molar productivity for DODH over C-supported ReO_x; which along with the above findings and our previous work on Pt-ReO_x/C, activated carbon emerged as an optimal support.[26,43] DODH of mucic acid (**1**) removes four hydroxyl groups (two pairs) and generates two C=C double bonds. In addition to DODH, esterification of the carboxylic acid groups

(-COOH) is possible in isopropanol, yielding not only muconic acid (**2-diacid**) but also monoisopropyl muconate (**2-monoester**), and diisopropyl muconate (**2-diester**). In a batch reactor, ReO_x/C catalyst showed 85% conversion of **1** in 6 h at 180°C, producing 66% yield of **2** (entry 1 in **Table 1**). As discussed elsewhere, isopropanol can serve as a reductant and donate dihydrogen for DODH, being converted to acetone as a byproduct.[26,29,30]

On the other hand, MoO_x/C and VO_x/C catalysts exhibited 66% and 55% conversion of **1**, respectively, under the same reaction conditions. However, DODH selectivity to the desired dialkene intermediate was quite low over both, wherein MoO_x/C attained 6% yield and VO_x/C just 1% yield of **2** (entry 2 and 3 in **Table 1**). Molybdenum and vanadium-based catalysts for DODH have been reported, yet insufficient activity was shown under 200°C.[29] However, at reaction temperatures over 200°C, conversion did increase but led to unwanted side reactions, particularly problematic for complex substrates like biomass derivatives.[29,31] Based on ^{1}H NMR chemical shifts (**Figure S1**), MoO_x/C and VO_x/C preferentially formed cyclic dehydration products, likely 5- or 6-membered lactones via intramolecular esterification ('Others', entry 2 and 3 in **Table 1**). Therefore, despite their decreased cost, low DODH activity and selectivity over MoO_x or VO_x catalysts make their usage as alternatives to ReO_x for DODH of **1** less attractive.

In addition to DODH, ReO_x/C has been shown to catalyze transfer hydrogenation in isopropanol.[26,30] In agreement, following the conversion of **1** to **2** over ReO_x/C, further conversion to 2% yield of 2-hexenedioic acid and its esters (**3**) and additional isomerization totaling 5% yield of 3-hexenedioic acid and its esters (**4**) was detected. Isopropanol has been widely employed as a hydrogen source for transfer hydrogenation.[32,33] Recently, H_2-free reduction over rhenium-based catalysts in light alcohols has been studied. Li et al. reported C–O bond cleavage of lignin model compounds over ReO_x/C with isopropanol as a hydrogen donor.[34] Similarly, our previous study demonstrated that transfer hydrogenation over ReO_x catalyst afforded the saturated products from C=C double bonds in isopropanol without H_2 gas.[26] Likozar et al. proposed a mechanism of H_2-free reduction in the presence of methanol as a hydrogen donor from DFT calculations. Methanol gives off the hydroxylic hydrogen on metallic rhenium and the hydroxylic hydrogen from methanol can then hydrogenate C=C double bonds.[25]

While the tandem reaction of DODH and CTH converted **1** to adipic acid (**5-diacid**) or adipates (**5-monoester** and **5-diester**), the reported yields of the tandem reaction with ReO_x alone were not satisfactory (30-35%).[25,26] The strategy of adding Pt or Pd catalysts to an oxophilic promoter (ReO_x) has been shown to significantly increase the rate of transfer hydrogenation. This, combined with the DODH ability of ReO_x, resulted in high yields of **5** (60-99%).[21,22,25,26] Despite the increased yields of **5**, the additional requirement of 2-3 wt% of a noble precious metal content with a high supply risk is a key challenge in the production of **5** from **1** at scale.

To this end, we prepared several M-ReO_x/C catalysts with 0.05 wt% of M via a co-impregnation method and evaluated their ability for both DODH and CTH reactions. The presence of 0.05 wt% Pt or Ni resulted in very low yield (2-3%) of CTH products **3**,**4**, and **5** (entry 4 and 5, **Table 1**). The addition of Pd resulted in the lowest observed conversion out of all catalysts screened and a poor yield of **2** with no hydrogenated products **3**,**4**, and **5** detected (entry 6). This is likely due in part to hindered DODH activity in the Pd-ReO_x/C catalyst via *in-situ* electronic deactivation. Pd has been reported to readily promote the reduction of Re^{n+} (ReO_x) into lower-valency $Re^{<n+}$ and Re^0, under reductive conditions.[35,36]. High oxidation states of Re (IV-VII) are considered to be the active species for DODH, and the reduction of these species to lower oxidation states by Pd might be responsible for the lower ReO_x DODH activity, resulting in the poor observed conversion of **1**.[20,26,37] Interestingly, with only 0.05 wt% rhodium, ruthenium, or iridium added to ReO_x/C, a significant amount of partially and fully hydrogenated products were produced from **1** (entry 7-9). Among them, Ir-ReO_x/C (4.33 wt% Re and 0.05 wt% Ir) stood out as the highest yields of hydrogenated products **3-5** compared to the other catalysts. Previously, high turnover frequency (TOF) of iridium catalyzed CTH with isopropanol as a hydrogen donor has been reported, and as a result Ir-based complexes have attracted much attention for the CTH reaction.[32] However, few heterogeneous iridium catalysts for CTH have been studied. Hermans et al. synthesized CeO_2 supported iridium oxide catalyst for CTH of cyclohexanone with 2-butanol as a hydrogen donor.[38] Crabtree and Hintermair et al. synthesized metallic Ir^0 nanoparticles and showed their high activity in the CTH of acetophenone with KOH additive.[39] Our initial findings supporting Ir in screening M-ReO_x/C coupled with encouraging past reports of high activity over Ir catalysts warranted further study of Ir-ReO_x/C. The ability of Ir to catalyze hydrogenation despite a low 0.05 wt% loading decreases the cost per mol product by considerably reducing the quantity of platinum-group metal (PGM) necessary for DODH-CTH (**Table S1**). In addition to the cost reduction in catalyst, breakthroughs to reduce the production cost of substrate and the operating and capital cost should be addressed in parallel to bolster the economic viability of this process.

Table 1. DODH-CTH tandem reaction of **1** over monometallic and bimetallic catalysts.[a]

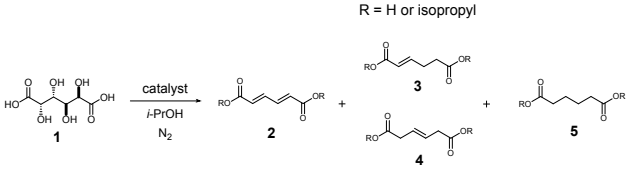

Entry	Catalyst (metal content, wt%)	Conv.[b] (%)	Products / % yield[b]				
			2	**3**	**4**	**5**	Others
1	ReO_x/C (Re 4.5)	85	66	2	5	0	12
2	MoO_x/C (Mo 4.5)	66	6	0	2	0	58

3	VO_x/C (V 4.5)	55	1	1	0	0	53
4	Pt-ReO_x/C (Pt 0.05, Re 4.5)	85	71	1	1	0	12
5	Ni-ReO_x/C (Ni 0.05, Re 4.5)	73	65	1	2	0	5
6	Pd-ReO_x/C (Pd 0.05, Re 4.5)	38	28	0	0	0	10
7	Rh-ReO_x/C (Rh 0.05, Re 4.5)	92	77	4	10	0	1
8	Ru-ReO_x/C (Ru 0.05, Re 4.5)	79	68	4	6	0	1
9	Ir-ReO_x/C (Ir 0.05, Re 4.5)	83	24	20	20	3	16

[a] Reaction conditions: batch reaction, 180°C, 6 h, catalyst (150mg), **1** (210 mg), *i*-PrOH (40 mL), and N_2 (15 bar).
[b] Conversion and yield are calculated by ^{1}H NMR.

3.2 DODH-CTH reaction over Ir-ReO_x/C. DODH-CTH of **1** by the Ir-ReO_x/C (4.33 wt% Re and 0.05 wt% Ir) was investigated at different temperatures (180-220°C) and shown in **Figure 2**. At 180°C, **1** was selectively converted to **2** in 1 h with a conversion of 60%. After 12 h, the conversion extent increased to 96%, and the resulting **2** was partially hydrogenated to **3**/**4**. An additional 12 h of reaction time (24 h at 180°C in **Figure 2**) converted **3**/**4** slowly to **5**, indicating the lower rate of the second hydrogenation step (**3**/**4** to **5**) to that of the first hydrogenation step (**2** to **3**/**4**). This is consistent with a recent modelling study of the hydrogenation of **2** to **5** wherein the first hydrogenation from **2** to **3** had lower activation energy than the second hydrogenation of **3** to **5**.[40] In addition to the kinetics, catalyst deactivation led to the reduced rate of secondary hydrogenation after 12 h. **Figure 2 (a)** shows a 24 h reaction in which the reaction was stopped and the catalyst was removed and replaced with new catalyst at 12 h. Compared to the 24 h reaction without interruption, replacement with new catalyst at 12 h produced more **5**, indicative of catalytic deactivation present in the 24 h, single catalyst system. Deactivation and regeneration of the catalyst are discussed in more detail in Section 3.5.

The rate of hydrogenation by the Ir-ReO_x/C catalyst was facilitated at higher temperatures, yielding a higher amount of **5**. The highest yield of **5** (63%) was obtained at 200°C after 48 h. At 220°C, all hydrogenation steps were completed in 24 h, giving **5** with a yield of 59%. The higher reaction temperature of 220°C also facilitated esterification, resulting in high selectivity (> 90%) to diisopropyl adipate (**5-diester**) in the mixture **5** (**Figure S2**). It was previously reported that a lower reaction temperature of 170°C with Pt-ReO_x/C produced adipic acid (**5-diacid**), monoisopropyl adipate (**5-monoester**), and **5-diester** with a similar distribution.[26] The reaction pathway, estimated by changes in ^{1}H NMR spectra over time, begins with two-fold DODH of **1** to **2**, followed by two sequential hydrogenation steps to **5** (**Figure S3**).

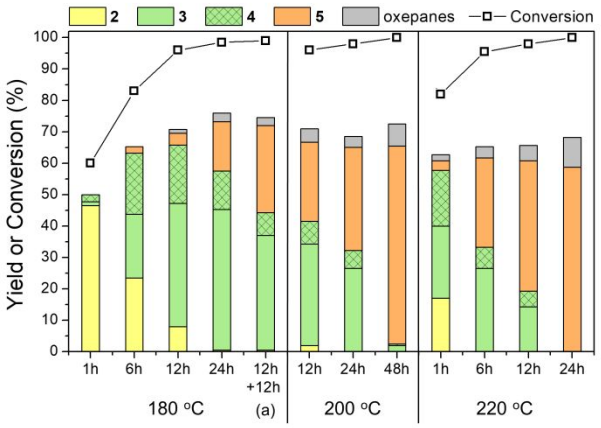

Figure 2. DODH-CTH by Ir-ReO_x/C. The secondary x-axis labels (below the time points) indicate the reaction temperature. Reaction conditions: batch reaction, Ir-ReO_x/C (150 mg, 4.33 wt% Re and 0.045 wt% Ir), **1** (210 mg, 1 mmol), N_2 (15 bar), isopropanol (40 mL). (a) After 12 h reaction, the catalyst was removed and fresh catalyst was added. Further 12 h reaction was conducted with the fresh catalyst. **Table S2** contains the quantitative information for the data shown here.

The extent of leaching of active species from Ir-ReO_x/C catalyst under reaction conditions was analyzed. Based on ICP analysis, the fresh Ir-ReO_x/C catalyst consists of 4.33 wt% of Re and 0.046 wt% Ir. After 6 h reaction at 220°C, both the content of Re and Ir decreased to 3.68 wt% and 0.036 wt%, respectively (**Figure 3A**), suggesting leaching of both Re and Ir. Sharkey and Jentoft reported rhenium diolate as leached species formed from condensation of vicinal diols with rhenium surface species during DODH reaction. The extent of leaching is highly dependent on the solubility of the formed rhenium diolate.[41] To alleviate leaching, higher thermal treatment temperatures in the catalyst synthesis step were employed. Higher thermal treatment temperature under N_2 could further reduce rhenium species due to the reductive properties of the carbon support.[42] If effective, the resulting lower oxidation states of rhenium species would be less soluble in organic solvents and therefore more resistant to leaching, but potentially less active in DODH, therefore an optimal balance between the two could exist.[41,43] When the thermal treatment temperature increased from 480°C to 530°C, the average oxidation state of Re slightly decreased (**Figure S5** and **Table S6**), and as a result ReO_x was not leached out during the reaction (**Figure 3A**). However, the increased reduction had a negative effect on the reaction, lowering conversion and product yields (**Figure 3B**), as was previously mentioned regarding Pd-ReO_x/C. The catalyst prepared at 580°C was stable under the reaction conditions, but a further decrease in conversion was observed. Thus, thermal treatment at 530°C was determined to be an optimal condition at which leaching is avoided while minimizing detrimental effects on reactivity.

Compared to the reaction with Ir-ReO_x/C treated at 480°C (denoted as Ir-ReO_x/C-480), Ir-ReO_x/C thermally treated at 530°C (denoted as Ir-ReO_x/C-530) showed a similar reaction profile, but slightly lower yield of **5** (**Table 2**). After 24 h, the yield of **5**

reached 50%. When the reaction substrate concentration increased from 0.025 M to 0.125 M while using the same substrate/catalyst ratio (1.4 g/g), a similar yield of **5** (53%) was obtained (entry 4 in **Table 2**), indicating that solvent is not a limiting reagent. This suggests the potential to reduce the solvent usage, which could be one of the cost drivers in this process.

The TGA profile of the fresh Ir-ReO_x/C-530 catalyst showed an initial 6 wt% weight loss at 50°C due to desorption of water in the catalyst (**Figure 4A**).[44] The carbon support started decomposition at 500°C, resulting in drastic weight loss in the profile from oxidation.[45] In addition to the weight losses due to the desorption of water and support decomposition, a notable weight loss of 5 wt% in the temperature between 200-350°C in the profile of the spent catalyst was observed, that did not occur for the fresh catalyst. This is most likely attributed to the organic deposits generated and deposited on the catalyst surface during the reaction.[46,47]

At the reaction temperatures (180-220°C), side reactions also yielded some byproducts. Cyclization followed by hydrogenation of **5** produced oxepane, a seven-membered cyclic ether, detected in NMR spectra (**Figure S3**). The NMR peaks corresponding to CH_3 groups (δ = 0.7-0.9) may include internally alkylated adipates and 2-propyl malonate.[48] Some of these side reactions can be limited by protecting the carboxylic acid group of **1** via Fischer esterification with isopropanol. Indeed, DODH-CTH reaction of the esterified **1**, diisopropyl mucate, (**1-diester**) as substrate, resulted in a reduced mass loss (15%) to unwanted side products and increased the rate of reaction (**Figure S4**). The conversion of isopropanol during DODH-CTH was measured (**Table S4**). The 6 h reaction at 220 °C exhibited 10% conversion of isopropanol, which is larger than previously reported conversion (5.5%) from DODH-CTH reaction at a lower temperature of 170 °C.[26] The major products from isopropanol include acetone (1.4 mmol) and diisopropyl ether (3.8 mmol), resulting in a C3 carbon balance of 91%.

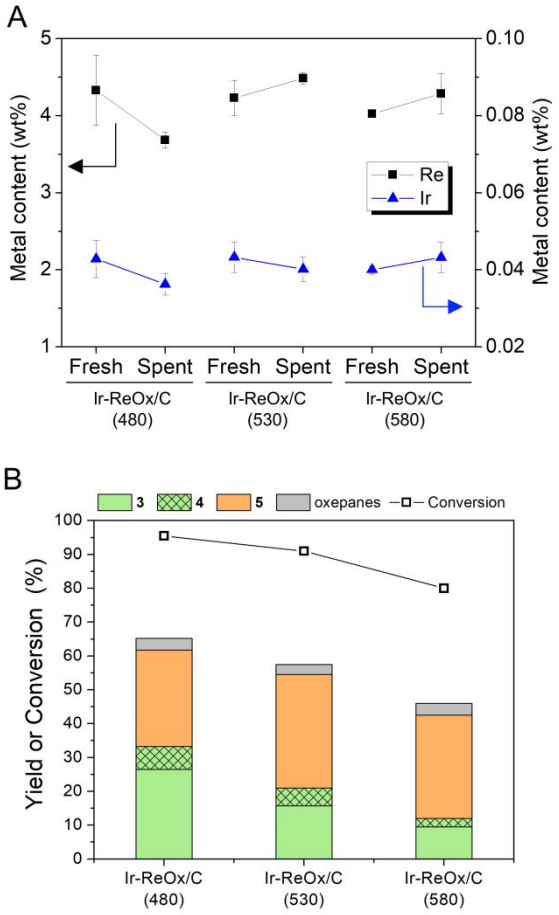

Figure 3. (A) metal contents measured by ICP-AES of fresh and spent Ir-ReO_x/C catalysts prepared in different thermal treatment temperatures (480, 530, and 580°C). **(B)** DODH-CTH over Ir-ReO_x/C catalysts treated at 480, 530, and 580°C. Reaction conditions: batch reaction, catalyst (150 mg), **1** (210 mg, 1 mmol), N_2 (15 bar), isopropanol (40 mL). **Table S3** contains the quantitative information for the data shown here.

Table 2. DODH-CTH Tandem Reaction of **1** over Ir-ReO_x/C-530.[a]

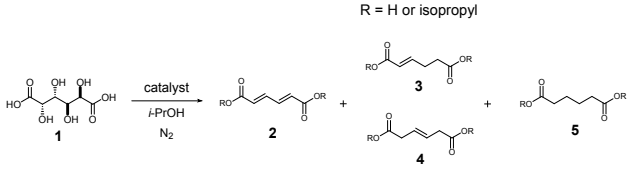

Entry	Time (h)	Conv.[b] (%)	Products / % yield[b]					
			2	**3**	**4**	**5**	Oxepane	Others
1	6	91	0	16	5	34	3	33
2	12	100	0	9	2	42	5	42
3	24	100	0	0	0	50	6	44
4[c]	24	100	0	0	0	53	5	42

[a] Reaction conditions: batch reaction, 220°C, Ir-ReO_x/C-530 (4.33 wt% Re and 0.046 wt% Ir, 150mg), **1** (210 mg), *i*-PrOH (40 mL), and N_2 (15 bar).
[b] Conversion and yield are calculated by ^{1}H NMR.
[c] 1.05 g of substrate (**1**) and 750 mg of Ir-ReO_x/C-530.

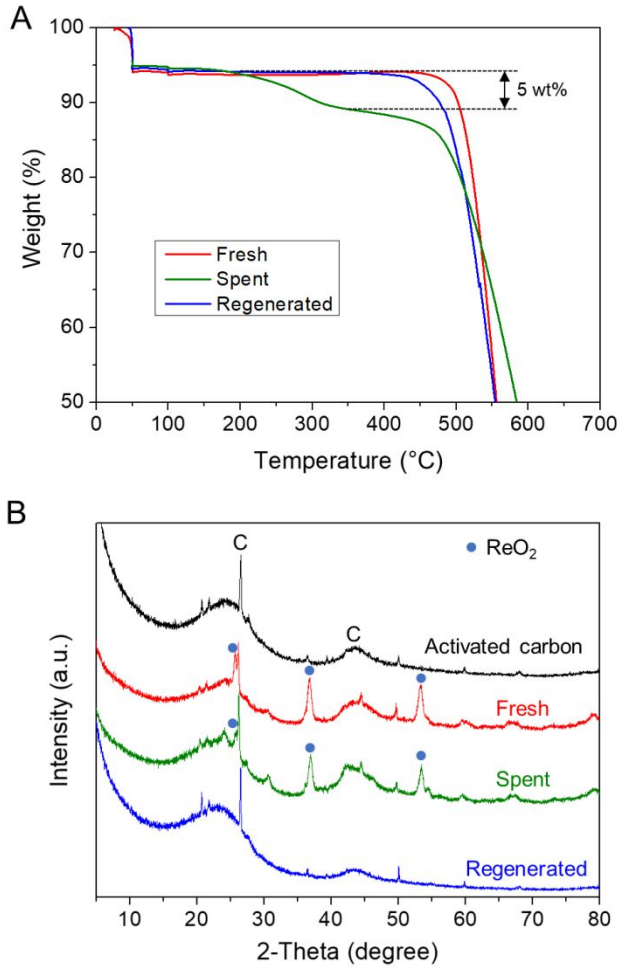

Figure 4. (A) TGA profiles of fresh, spent, and regenerated Ir-ReO_x/C-530. **(B)** XRD diffractograms of activated carbon, fresh, spent, and regenerated Ir-ReO_x/C-530. Peaks with blue circles indicate ReO_2.

3.3 Catalyst characterization. The fresh and spent Ir-ReO_x/C-530 catalysts were characterized. XPS analysis was performed to examine the valance states of Re and Ir in the fresh Ir-ReO_x/C-530 catalyst. The results are displayed in **Figure 5** and **Table S6**. The curve-fitted Re 4f spectra suggest Re^{VII} (60%) at binding energies 44.7 and 47.1 eV as the primary oxidation state.[49,50] 21% of Re^{IV} ($4f_{7/2}$ peak at 42.2 eV) and 8% of metallic Re ($4f_{7/2}$ peak at 40.8 eV) were also detected, indicating the reduction of ammonium perrhenate (VII) precursor during synthesis. For the Ir 4f spectra, we note that due to very low Ir content (0.046 wt%), XPS peaks are relatively small and less resolved than Re. Binding energies at 61.9 and 64.9 eV represent Ir(IV)O_2.[51,52] No precursor species (Ir(III)Cl_3, $4f_{7/2}$ peak at 62.5 eV) was measured, showing that the precursor was converted into the oxide during the catalyst preparation, in an analogous fashion to Re.

The oxidation states of Re and Ir, psuedo *in-situ* and after DODH-CTH, were investigated to identify the involved species. To measure oxidation states of the active species under the reaction conditions, the catalyst after 24 h reaction at 220°C was separated in an inert gas-filled glove box and transferred to the XPS chamber without exposure to atmosphere. Under the reaction conditions, Re^{VII} in the fresh catalyst was significantly reduced to Re^{VI} (36%), Re^{IV} (12%), and metallic Re^0 (38%). Previously, we demonstrated that Re^{VI} and Re^{IV} are the dominant species for Pt-ReO_x/C during DODH and that metallic Re^0 was not active for DODH.[26] Consistently, the detected Re^{VI} and Re^{IV} in Ir-ReO_x/C are also the likely active species for DODH. In addition, the disappearance of Ir^{IV} and the appearance of metallic Ir^0 ($4f_{7/2}$ peak at 60.9 eV) during the reaction suggest metallic Ir^0 as an active phase for CTH. After the reaction, when the catalyst was exposed to air ("spent" sample in **Figure 5**), both Re and Ir were re-oxidized to similar oxidation states of the fresh Ir-ReO_x/C-530 catalyst.

In the XRD pattern of the fresh catalyst, peaks of carbon support and ReO_2 were observed (**Figure 4B**). No crystalline phase corresponding to Re^{VII} species was observed even though Re^{VII} is the major Re species detected by XPS analysis, indicating the Re^{VII} species are likely amorphous. There were no peaks for Ir species because Ir species are highly dispersed and/or because the concentration of Ir is too low. STEM analysis of the fresh catalyst revealed that the particle size ranged from 3 to 12 nm, estimating the average particle size of 5.8 ± 1.7 nm (**Figure S6**).

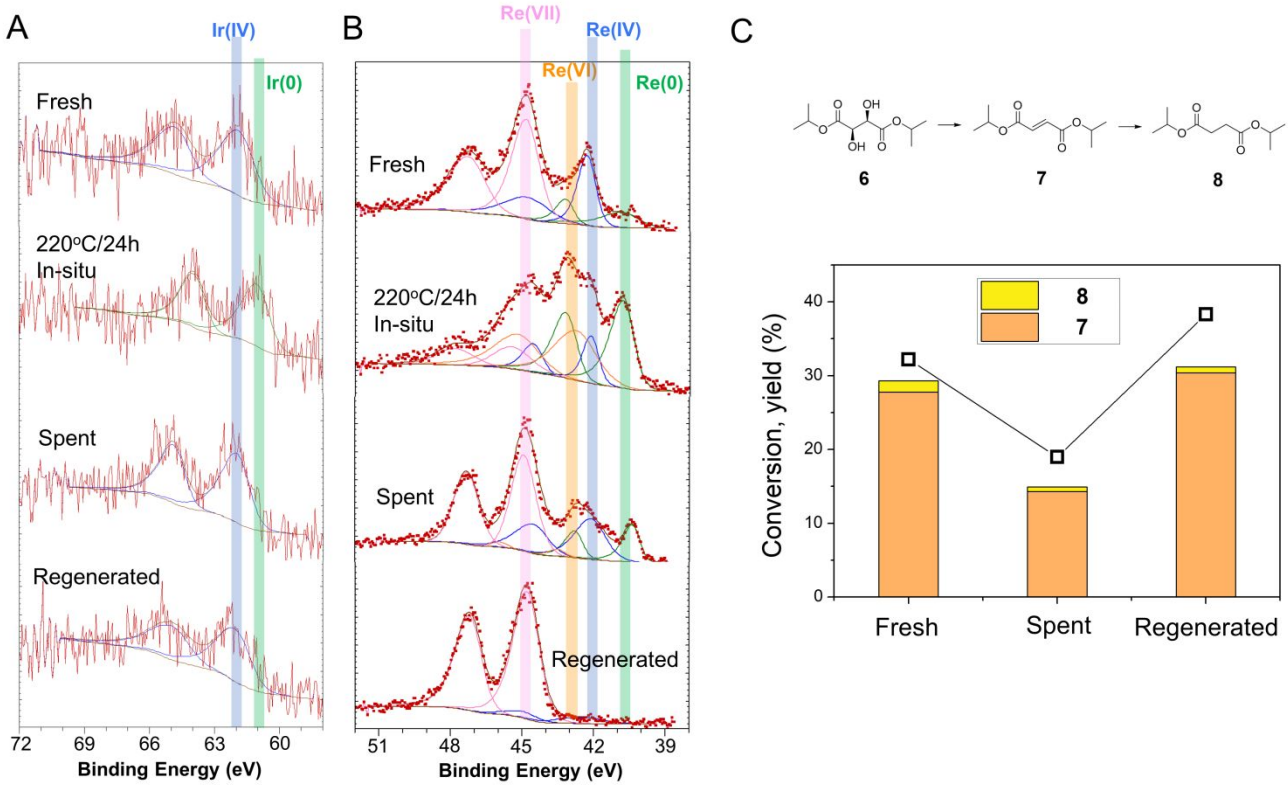

Figure 5. Changes in XPS spectra **(A)** Ir 4f and **(B)** Re 4f in Ir-ReO_x/C-530 catalyst over reaction and regeneration. *In-situ* 24 h sample under the reaction conditions were analyzed without air exposure. After 24 h reaction, the spent catalyst was prepared by washing and drying in a 120°C oven. The spent catalyst was regenerated at 300°C under air for 4 h. **(C)** Activity test of the fresh, spent, and regenerated catalysts. Reaction conditions: 1 mmol diisopropyl-L-(+)-tartrate (**6**), 150 mg Ir-ReO_x/C-530, 10 mL isopropanol, 220°C, 20 min reaction and 25 min heating ramp. **Table S6** contains the quantitative information for the XPS data shown here.

3.4 Catalyst deactivation and regeneration. The stability and reusability of the Ir-ReO_x/C-530 catalyst was investigated. To compare the activity of the fresh and spent catalyst for DODH, diisopropyl L-(+)-tartrate (**6**) was used as a model substrate for experimental and analytical convenience (**Figure 5C**) as mentioned in Section 2.4. At 220°C, fresh Ir-ReO_x/C-530 catalyst converted 32% of **6** in 20 min, producing **7** and **8** (27% and 2% yields, respectively). The recovered catalyst ("spent" in **Figure 5C**) exhibited lower conversion (19%) and yield of **8** (14%). Given the similar oxidation states (**Figure 5A-B**) and Re + Ir metal contents (**Figure 3A**) of the spent catalyst relative to those of the fresh catalyst, the reduced DODH activity is mostly due to organic deposits via coke deposition on the catalyst as detected by TGA (**Figure 4A**). It is worth noting that ReO_2 peaks in the XRD diffractogram of the spent catalyst disappeared after regeneration, possibly because of a phase change to an amorphous state (**Figure 4B**).

The catalyst deactivated via coke deposition could be regenerated by removing the organic deposits through thermal treatment under oxidative conditions.[53,54] The spent Ir-ReO_x/C-530 catalyst was thermally treated at 300°C for 4 h under flowing air. The thermal regeneration temperature was determined from TGA results that indicated that 300°C was sufficient to remove organic deposits but low enough to limit decomposition of the carbon support (**Figure 4A**). The TGA profile of the regenerated catalyst did not show weight loss in the temperature between 200-350°C, clearly indicative of the removal of deposited organic material. During the regeneration step at 300°C, a 6% mass loss was observed, which is mostly due to the removal of organic deposits (5 wt% of the spent catalyst) during thermal treatment (**Figure S7**). This observation suggests that the carbon support was stable at 300°C. However, regeneration at 350°C and especially 400°C resulted in more significant mass reduction (11 wt% and 66 wt%, respectively), from oxidation of the carbon support.

The catalyst regenerated at 300°C exhibited an increase in the conversion to 38% with a 30% yield of **7**, which are higher than the values obtained from the reaction with the fresh catalyst (**Figure 5C**). This is because regeneration further oxidized lower valent rhenium to species with higher DODH activity (**Figure 5A**) as well as serving to remove organic deposits accumulated from the reaction. Accordingly, the regenerated catalyst consisted of Re^{VII} (92%), Re^{IV} (8%), with no metallic Re observed, in contrast to 60% Re^{VII}, Re^{IV} (21%), and 8% Re^0 species in the fresh Ir-ReO_x/C catalyst.

For evaluation of catalyst recyclability in the reaction to adipates, mucic acid (**1**) was used as substrate and displayed good reuse upon regeneration in at least three cycles (**Table 3**). It should be noted that we conducted the recycling test at incomplete conversions to avoid obscuring protential deactivation.[55] In comparison to fresh catalyst (entry 1), the conversion and

selectivities following oxidative regeneration were altered. Conversion of **1** increased from 60% in the fresh catalyst to 82% following regeneration as oxidation of Re species increased DODH activity as previously mentioned in the reaction of **6**. Consistently, the regenerated catalysts exhibited a higher conversion of isopropanol, producing more acetone and diisopropyl ether relative to the fresh catalyst (**Table S5**). However, this oxidative treatment negatively impacted Ir hydrogenation as the yield of partially (**3**-**4**) and fully saturated (**5**) species over the regenerated catalysts decreased from 43% over fresh catalyst, to 17% and 8% following the first and second regenerations, respectively (entry 2 and 3, **Table 3**). To confirm the altered conversion and product yield were due to oxidation of Re and Ir, the fresh catalyst was subjected to the same treatment used for regeneration (entry 4) and exhibited similar conversion and product yield to those over the regenerated spent catalyst (entry 2, **Table 3**).

In order to probe catalyst recycling with and without regeneration and Ir-ReO_x/C-530 long-term stability, multiple consecutive runs of DODH of **6** were conducted by reusing the catalyst (**Figure 6**). We note that **7** was a dominant product with a very small amount of **8** at the tested conversion level (**Figure 5C**). Without the regeneration step, the conversion steadily decreased from 38% to 11% in four cycles possibly due to catalyst fouling from increasing accumulation of organic matter. After the 4th cycle, the catalyst was regenerated at 300°C and tested for a 5th cycle. The regeneration step increased the conversion to 28%, indicating partially recovered activity of the catalyst. After the 5th and 6th runs, the catalyst was regenerated and the conversion was maintained at 24%. Conversely, when the regeneration step was instead employed after each cycle, the conversion was maintained between 34-42% up to five cycles, demonstrating the effectiveness of the regeneration conditions.

Table 3. Recycling Studies of **1** over Ir-ReO_x/C-530.[a]

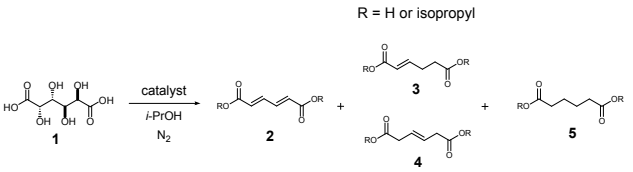

Entry	Catalyst	Conv.[b] (%)	Products / % yield[b]				
			2	**3**	**4**	**5**	Others
1[a]	Ir-ReO_x/C-530	60	14	24	16	3	3
2	2nd Cycle[c]	82	61	7	9	1	4
3	3rd Cycle[c]	85	69	3	4	1	7
4	Ir-ReO_x/C-530[d]	83	57	9	10	1	6

[a] Reaction conditions: 220°C, 30 min, Ir-ReO_x/C-530 (4.33 wt% Re and 0.046 wt% Ir, 150mg), **1** (210 mg), *i*-PrOH (40 mL), and N_2 (15 bar).
[b] Conversion and yield are calculated by ^{1}H NMR.
[c] Regeneration conditions: 300°C, 4 h, under flowing air. Regeneration experiments were scaled down to maintain the catalyst/substrate ratio.
[d] Fresh catalyst subjected to regeneration conditions.

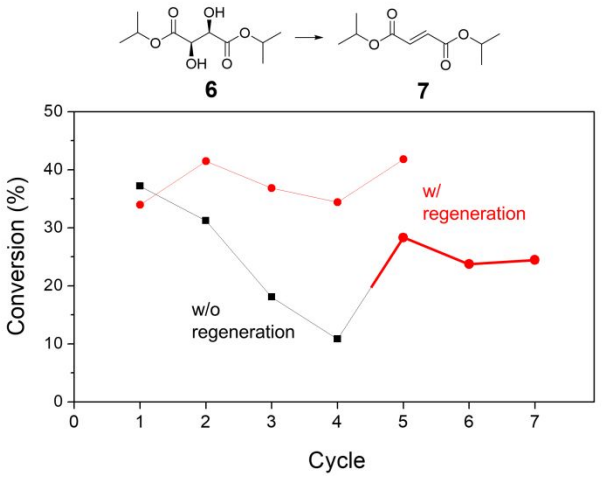

Figure 6. Stability test of Ir-ReO_x/C-530. Reaction conditions: 1 mmol diisopropyl-L-(+)-tartrate (**6**), 150 mg catalyst, 10 mL isopropanol, 220°C, 20 min reaction and 25 min heating ramp. Regeneration conditions: flowing air, 300°C, and 4 h.

3.5 Mechanism. The transfer hydrogenation ability of Ir-ReO_x/C-530, ReO_x/C, and a physical mixture of Ir/C and ReO_x/C were examined (**Figure 7**) to determine the capacity of each species in CTH and evaluate possible synergy. Though not a typical hydrogenation catalyst, even in high oxidation states as ReO_x, Re has been reported active in alkene saturation, and therefore elucidation of its CTH activity in the present system was necessary.[56] Diisopropyl fumarate (**7**) was used as a model compound for transfer hydrogenation of the C=C double bond in **7**, producing diisopropyl succinate (**8**). Without the presence of iridium, ReO_x/C (4.33 wt%, 150 mg) gave a 15 % yield of **8** in 1 h at 160°C in agreement with previous observations that ReO_x alone catalyzed transfer hydrogenation of C=C double bonds in isopropanol.[25,26,30] Ir-ReO_x/C-530 (4.33 wt% Re and 0.046 wt% Ir, 150 mg) catalyst exhibited a 34% yield of **8**, nearly twice the yield achieved by ReO_x/C alone. This proves that transfer hydrogenation was notably promoted by the addition of iridium despite its very low content of 0.046 wt% (0.042 mol%) especially when compared to the 4.33 wt% loading of Re (3.49 mol%). To clarify whether the metallic interface of Ir and Re plays a vital role in CTH, a physical mixture of Ir/C (0.05 wt%, 150 mg) and ReO_x/C (4.33 wt%, 150 mg) was also examined. A physical mixture produced a 38% yield of **8**. The similar activity between the Ir-ReO_x/C-530 catalyst and the physical mixture indicates that CTH occurred on individual Ir and Re sites rather than on the interface of Ir-Re. In addition, the promoted activity for hydrogenation by the physical mixture wherein Ir sites are separated from ReO_x sites precludes the possibility of hydrogen spillover between Ir and ReO_x sites as a dominant mechanism of hydrogenation. All the observations are consistent with the previously proposed bifunctional mechanism of DODH-CTH; DODH occurs on Re and CTH reaction is promoted by the addition of platinum-group metals.[26] A widely accepted DODH mechanism includes formation of rhenium-diolate (condensation), reduction of the rhenium diolate, and alkene release via extrusion with redox pairs of Re^{VI}/Re^{IV} or Re^{VII}/Re^{V}.[35,37,43] Similarly, the DODH mechanism

by Ir-ReO_x/C catalyst included Re^{VI} and Re^{IV}, detected by XPS analysis under the reaction conditions. Isopropanol provided dihydrogen to reduce the rhenium diolate, making acetone as a byproduct. Two consecutive DODH cycles could convert **1** to **2**. Previously, we reported hot-filtration experiments in a similar catalytic system, demonstrating that DODH of **1** to **2** over ReO_x proceeded on the heterogeneous surface, not by solubilized molecular species, thus homogeneous DODH was assumed to be negligible under the tested reaction conditions.[26] The resulting double bonds were hydrogenated to **3-5** via CTH primarily over metallic Ir^0 (**Scheme 2**).

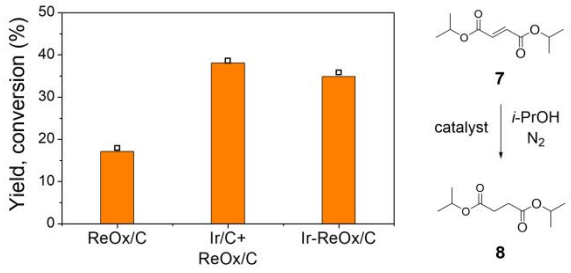

Figure 7. CTH reaction over ReO_x/C, physical mixture of Ir/C and ReO_x/C, and Ir-ReO_x/C-530. Reaction conditions: 1 mmol diisopropyl-fumarate (**7**), 10 mL isopropanol, 160°C, 1 h reaction and 15 min heating ramp.

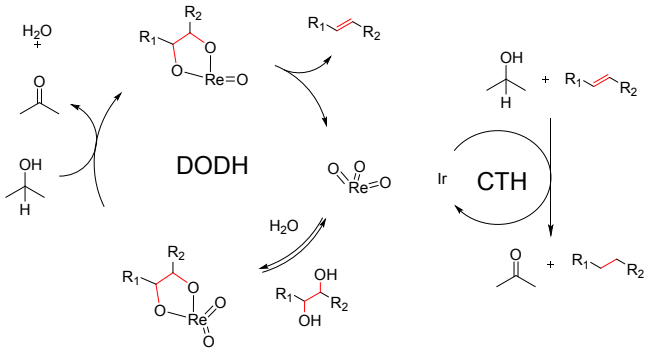

Scheme 2. Proposed mechanism of DODH-CTH over Ir-ReO_x/C.

Conclusions

Bifunctional Ir-ReO_x/C catalysts with low Ir loading were synthesized for tandem DODH-CTH of mucic acid and revealed production of the corresponding adipate in good yield. Compared to its monometallic ReO_x/C counterpart, a marked improvement in transfer hydrogenation ability, and thus yield of adipates, was found over Ir-ReO_x/C despite limited Ir loading of 0.046 wt%. Isopropanol was shown to function as *in-situ* hydrogen source, solvent, and catalytic reductant for DODH as well as CTH. The optimum selectivity to adipates reached 66% with near-complete conversion (63% yield, 96% conversion) in a one-step batch reaction at 200°C for 48 h. Loss of catalyst activity was observed through recycling and stability tests, and in conjunction with TGA and XPS analysis, was determined to arise primarily from deposition of organic matter on the catalyst surface, blocking active sites. Optimization of regeneration conditions was conducted to prevent oxidation of the carbon support while effectively removing catalyst coking, the specific conditions of which were found to further increase catalytic activity, confirmed by XPS analysis which maximized high-valent Re population, supporting findings that these species are the most active in DODH. Regeneration tests enabled the recycled Ir-ReO_x/C catalyst to sustain the activity of the fresh catalyst at a conversion level between 34-42% for at least five cycles. A bifunctional DODH-CTH mechanism was presented based on reactions of model substrates and spectroscopy.

Author Contributions

JHJ: Conceptualization, Methodology, Validation, Formal analysis, Investigation, Resources, Data curation, Visualization, Writing – original draft, Writing – review & editing. **JTH:** Methodology, Validation, Formal analysis, Investigation, Resources, Data curation, Visualization, Writing – original draft, Writing – review & editing. **IR:** Validation, Writing – review & editing. **PC:** Conceptualization, Methodology, Writing – review & editing, Supervision, Funding acquisition. **MMAO:** Conceptualization, Methodology, Resources, Data curation, Writing – review & editing, Supervision, Funding acquisition, Project administration. All authors approved the final version of the manuscript.

Conflicts of interest

There are no conflicts to declare.

Acknowledgements

This work was supported by the US Department of Energy, Office of Science, Basic Energy Science, Award No. DE-SC0019161 (M.M.A.-O.). The use of ICP, STEM, XRD, and XPS equipment in the UCSB Materials Research Laboratory was supported by the MRSEC Program of the National Science Foundation under Award No. DMR 1720256. This work was supported in part by NIH Shared Instrumentation Grant, S10OD012077, for magnetic resonance instrumentation. Dr. Baoyuan Liu is acknowledged for assistance with ICP analysis.

Notes and references

1 W. Ding, H. Li, R. Zong, J. Jiang and X. Tang, *ACS Sustain. Chem. Eng.*, **2021**, *9*, 3498–3508.
2 L. Wu, T. Moteki, A. A. Gokhale, D. W. Flaherty and F. D. Toste, *Chem*, **2016**, *1*, 32–58.
3 E. Skoog, J. H. Shin, V. Saez-Jimenez, V. Mapelli and L. Olsson, *Biotechnol. Adv.*, **2018**, *36*, 2248–2263.
4 R. Veski and S. Veski, *Oil Shale*, **2019**, *36*, 76.
5 J. C. J. Bart and S. Cavallaro, *Ind. Eng. Chem. Res.*, **2015**, *54*, 1–46.
6 J. Rios, J. Lebeau, T. Yang, S. Li and M. D. Lynch, *Green Chem.*, **2021**, *23*, 3172–3190.
7 W. Deng, L. Yan, B. Wang, Q. Zhang, H. Song, S. Wang, Q. Zhang and Y. Wang, *Angew. Chem. Int. Ed.*, **2021**, *60*, 4712–4719.

8 B. M. Stadler, C. Wulf, T. Werner, S. Tin and J. G. de Vries, *ACS Catal.*, **2019**, *9*, 8012–8067.
9 M. H. Thiemens and W. C. Trogler, *Science*, **1991**, *251*, 932–934.
10 *Inventory of U.S. Greenhouse Gas Emissions and Sinks: 1990-2015*, US Environmental Protection Agency, Washington, DC, 2017.
11 C. Weber, C. Brückner, S. Weinreb, C. Lehr, C. Essl and E. Boles, *Appl. Environ. Microbiol.*, **2012**, *78*, 8421–8430.
12 D. R. Vardon, M. A. Franden, C. W. Johnson, E. M. Karp, M. T. Guarnieri, J. G. Linger, M. J. Salm, T. J. Strathmann and G. T. Beckham, *Energy Environ. Sci.*, **2015**, *8*, 617–628.
13 L. Wei, J. Zhang, W. Deng, S. Xie, Q. Zhang and Y. Wang, *Chem. Commun.*, **2019**, *55*, 8013–8016.
14 M. J. Gilkey, H. J. Cho, B. M. Murphy, J. Wu, D. G. Vlachos and B. Xu, *ACS Appl. Energy Mater.*, **2020**, *3*, 99–105.
15 M. J. Gilkey, A. V. Mironenko, D. G. Vlachos and B. Xu, *ACS Catal.*, **2017**, *7*, 6619–6634.
16 Boussie, T. R.; Dias, E. L.; Fresco, Z. M.; Murphy, V. J., Production of Adipic Acid and Derivatives from Carbohydrate-Containing Materials. US 20100317822, June 2010.
17 R. T. Larson, A. Samant, J. Chen, W. Lee, M. A. Bohn, D. M. Ohlmann, S. J. Zuend and F. D. Toste, *J. Am. Chem. Soc.*, **2017**, *139*, 14001–14004.
18 M. Lang and H. Li, *ChemSusChem*, **2022**, *15*, e202101531.
19 H. Zhang, X. Li, X. Su, E. L. Ang, Y. Zhang and H. Zhao, *ChemCatChem*, **2016**, *8*, 1500–1506.
20 J. R. Dethlefsen and P. Fristrup, *ChemSusChem*, **2015**, *8*, 767–775.
21 M. Shiramizu and F. D. Toste, *Angew Chem. Int. Ed.*, **2013**, *52*, 12905–12909.
22 X. Li, D. Wu, T. Lu, G. Yi, H. Su and Y. Zhang, *Angew. Chem. Int. Ed.*, **2014**, *53*, 4200–4204.
23 S. Gunukula and R. P. Anex, *Biofuels Bioprod. Biorefining*, **2017**, *11*, 897–907.
24 L. J. Donnelly, S. P. Thomas and J. B. Love, *Chem. – Asian J.*, **2019**, *14*, 3782–3790.
25 B. Hocevar, A. Prasnikar, M. Hus, M. Grilc and B. Likozar, *Angew. Chem. Int. Ed.*, **2021**, *60*, 1244–1253.
26 J. H. Jang, I. Ro, P. Christopher and M. M. Abu-Omar, *ACS Catal.*, **2021**, *11*, 95–109.
27 N. N. Tshibalonza and J.-C. M. Monbaliu, *Green Chem.*, **2020**, *22*, 4801–4848.
28 A. R. Petersen and P. Fristrup, *Chemistry*, **2017**, *23*, 10235–10243.
29 J. R. Dethlefsen, D. Lupp, A. Teshome, L. B. Nielsen and P. Fristrup, *ACS Catal.*, **2015**, *5*, 3638–3647.
30 J. H. Jang and M. M. Abu-Omar, *Energies*, **2020**, *13*, 6402.
31 J. R. Dethlefsen, D. Lupp, B. C. Oh and P. Fristrup, *ChemSusChem*, **2014**, *7*, 425–8.
32 D. Wang and D. Astruc, *Chem Rev*, **2015**, *115*, 6621–86.
33 F. Alonso, P. Riente and M. Yus, *Acc. Chem. Res.*, **2011**, *44*, 379–391.
34 B. Zhang, Z. Qi, X. Li, J. Ji, L. Zhang, H. Wang, X. Liu and C. Li, *Green Chem.*, **2019**, *21*, 5556–5564.
35 N. Ota, M. Tamura, Y. Nakagawa, K. Okumura and K. Tomishige, *ACS Catal.*, **2016**, *6*, 3213–3226.
36 Y. Takeda, M. Tamura, Y. Nakagawa, K. Okumura and K. Tomishige, *ACS Catal.*, **2015**, *5*, 7034–7047.
37 J. H. Jang, H. Sohn, J. Camacho-Bunquin, D. Yang, C. Y. Park, M. Delferro and M. M. Abu-Omar, *ACS Sustain. Chem. Eng.*, **2019**, *7*, 11438–11447.
38 C. Hammond, M. T. Schümperli, S. Conrad and I. Hermans, *ChemCatChem*, **2013**, *5*, 2983–2990.
39 U. Hintermair, J. Campos, T. P. Brewster, L. M. Pratt, N. D. Schley and R. H. Crabtree, *ACS Catal.*, **2013**, *4*, 99–108.
40 A. Rosengart, C. Pirola and S. Capelli, *Processes*, **2020**, *8*, 929.
41 B. E. Sharkey and F. C. Jentoft, *ACS Catal.*, **2019**, *9*, 11317–11328.
42 S. R. de Miguel, O. A. Scelza, M. C. Román-Martínez, C. Salinas-Martınez de Lecea, D. Cazorla-Amorós and A. Linares-Solano, *Appl. Catal. A* **1998**, *170*, 93–103.
43 L. Sandbrink, E. Klindtworth, H.-U. Islam, A. M. Beale and R. Palkovits, *ACS Catal.*, **2016**, *6*, 677–680.
44 P. Veerakumar, N. Dhenadhayalan, K.-C. Lin and S.-B. Liu, *J. Mater. Chem. A*, **2015**, *3*, 23448–23457.
45 P. Veerakumar, I. Panneer Muthuselvam, C.-T. Hung, K.-C. Lin, F.-C. Chou and S.-B. Liu, *ACS Sustain. Chem. Eng.*, **2016**, *4*, 6772–6782.
46 M. A. Goula, A. A. Lemonidou and A. M. Efstathiou, *J. Catal.*, **1996**, *161*, 626–640.
47 N. D. Charisiou, L. Tzounis, V. Sebastian, S. J. Hinder, M. A. Baker, K. Polychronopoulou and M. A. Goula, *Appl. Surf. Sci.*, **2019**, *474*, 42–56.
48 X. She, H. M. Brown, X. Zhang, B. K. Ahring and Y. Wang, *ChemSusChem*, **2011**, *4*, 1071–1073.
49 M. T. Greiner, T. C. R. Rocha, B. Johnson, A. Klyushin, A. Knop-Gericke and R. Schlögl, *Z. Für Phys. Chem.*, **2014**, *228*, 521–541.
50 N. Ota, M. Tamura, Y. Nakagawa, K. Okumura and K. Tomishige, *ACS Catal.*, **2016**, *6*, 3213–3226.
51 D. Weber, L. M. Schoop, D. Wurmbrand, J. Nuss, E. M. Seibel, F. F. Tafti, H. Ji, R. J. Cava, R. E. Dinnebier and B. V. Lotsch, *Chem. Mater.*, **2017**, *29*, 8338–8345.
52 S. J. Freakley, J. Ruiz-Esquius and D. J. Morgan, *Surf. Interface Anal.*, **2017**, *49*, 794–799.
53 S. Vitolo, B. Bresci, M. Seggiani and M. G. Gallo, *Fuel*, **2001**, *80*, 17–26.
54 E. Heracleous, E. Pachatouridou, A. M. Hernández-Giménez, H. Hernando, T. Fakin, A. L. Paioni, M. Baldus, D. P. Serrano, P. C. A. Bruijnincx, B. M. Weckhuysen and A. A. Lappas, *J. Catal.*, **2019**, *380*, 108–122.
55 Scott, S. L. *ACS Catal.*, **2018**, *8*, 8597-8599.
56 T. Wang, M. Tamura, Y. Nakagawa and K. Tomishige, *ChemSusChem*, **2019**, *12*, 3615–3626.